# Neurogenesis of corticospinal motor neurons extending spinal projections in adult mice

**Jinhui Chen*, Sanjay S. P. Magavi, and Jeffrey D. Macklis†**

Departments of Neurosurgery and Neurology and Program in Neuroscience, Massachusetts General Hospital–Harvard Medical School Center for Nervous System Repair, Harvard Medical School, Massachusetts General Hospital, Boston, MA 02114

Communicated by Richard L. Sidman, Harvard Medical School, Boston, MA, September 15, 2004 (received for review March 17, 2004)

**The adult mammalian CNS shows a very limited capacity to regenerate after injury. However, endogenous precursors, or stem cells, provide a potential source of new neurons in the adult brain. Here, we induce the birth of new corticospinal motor neurons (CSMN), the CNS neurons that die in motor neuron degenerative diseases, including amyotrophic lateral sclerosis, and that cause loss of motor function in spinal cord injury. We induced synchronous apoptotic degeneration of CSMN and examined the fates of newborn cells arising from endogenous precursors, using markers for DNA replication, neuroblast migration, and progressive neuronal differentiation, combined with retrograde labeling from the spinal cord. We observed neuroblasts entering the neocortex and progressively differentiating into mature pyramidal neurons in cortical layer V. We found 20–30 new neurons per mm³ in experimental mice vs. 0 in controls. A subset of these newborn neurons projected axons into the spinal cord and survived >56 weeks. These results demonstrate that endogenous precursors can differentiate into even highly complex long-projection CSMN in the adult mammalian brain and send new projections to spinal cord targets, suggesting that molecular manipulation of endogenous neural precursors *in situ* may offer future therapeutic possibilities for motor neuron degenerative disease and spinal cord injury.**

The identification of populations of neural precursors, or stem cells, in the adult mammalian CNS raises the possibility of future repair of neuronal loss from neurodegenerative diseases or neuronal damage from brain and spinal cord injuries resulting from trauma or stroke (1–5). In the adult brain, new neurons are continuously generated, but such neurogenesis is normally restricted to two evolutionarily primitive regions: the olfactory bulb, from precursors in the subventricular zone (SVZ) (6), and the hippocampal dentate gyrus (1, 7), from local precursors in the subgranular zone.

A variety of factors, ranging from genetics (8) to environmental modifications, can modulate neurogenesis in these regions. Exercise (9), environmental enrichment (10), pregnancy (11), and even seizure activity (12, 13) promote neurogenesis, whereas depression (14) and aging (15) reduce it. Modulating the cellular and molecular factors that control adult neurogenesis could yield new approaches to replacing neurons lost to injury or disease.

Recently, our laboratory and those of others have demonstrated that neurogenesis can be induced from endogenous precursors by manipulating the microenvironment in regions of the adult CNS that are normally nonneurogenic (16–21). Selective neuronal death due to targeted apoptosis or ischemia induces endogenous precursors to divide and differentiate into neurons in mammalian neocortical layer VI (16), hippocampal region CA1 (17), striatum (18, 19), substantia nigra (20), and the high vocal center in songbirds (21). These neurons express neuron-specific proteins and adopt appropriate morphologies, and in some cases their recruitment correlates with restoration of function (17, 21). However, questions with significant clinical implications remain: Can neurogenesis be induced in regions of the brain further from the precursor-rich SVZ? Is it possible to induce the birth of very complex corticospinal motor neurons (CSMN) from endogenous precursors in adults, and can they reform and maintain extremely long-distance corticospinal projections affected by spinal cord injury and CSMN degenerations?

## Methods

This study is based on data from C57BL/6 adult female mice, which were used according to an institutionally approved protocol. CSMN in the adult mouse cortex were targeted for apoptotic cell death via chromophore photoactivation. Then, mice were administered BrdUrd for the 2 weeks after the induction of apoptosis, and the fate of BrdUrd+ cells was examined after 2-, 4-, 8-, 12-, 16-, and 56-week survival times by using morphological and immunocytochemical markers of progressive neuronal and glial differentiation. We examined projections formed by newborn neurons using the retrograde label FluoroGold (FG), injected at cervical C2–C3 at 7, 11, 15, and 55 weeks, and examined 1 week later.

**Targeted Neuronal Degeneration.** Details of chlorin $e_6$ injection and exposure to long-wavelength laser light have been described (16, 22, 23). In summary, a suspension of chlorin $e_6$-conjugated fluorescent nanospheres was injected bilaterally into the dorsal spinal cord at the cervical C5–C6 level of 4-week-old female mice, from which they were retrogradely transported to the somata of layer V CSMN in the motor cortex, where they remain inert until photoactivated. The nanospheres fluoresce in the same range as FITC, allowing unambiguous identification of targeted neurons (Fig. 1 *E–I*). Two weeks later, the motor cortex was exposed to 674-nm long-wavelength light through intact dura, photoactivating the chlorin $e_6$ to produce singlet oxygen and induce synchronous apoptosis (24) exclusively in nanosphere-containing motor neurons in the light-exposed region. Surrounding glia and unlabeled neurons remain intact. Degeneration of ≈10–20% of targeted projection neurons occurred, with neuronal degeneration confirmed in previous studies by loss of retrogradely labeled neurons compared with adjacent control regions and by the presence of terminal deoxynucleotidyltransferase-mediated dUTP nick end labeling-positive nuclei in projection neurons, confirming apoptotic death.

**BrdUrd Labeling of Dividing Cells.** We gave experimental and control mice drinking water containing BrdUrd (2.5 mg/ml) for 2 weeks after induction of apoptosis (approximate dose, 180 mg/kg per day). BrdUrd (Sigma) incorporates into dividing cells during S phase.

**Immunocytochemistry.** Four percent paraformaldehyde-fixed brain sections were washed in PBS and incubated with 2 M HCl for 2 h at room temperature. Then, the sections were blocked in PBS containing 4% goat serum, 0.3% BSA, and 0.3% Triton X-100 and incubated with primary antibodies overnight and with secondary antibodies for 2 h in blocking solution. We incubated the sections

Abbreviations: CSMN, corticospinal motor neuron(s); SVZ, subventricular zone; FG, FluoroGold; Dcx, Doublecortin; GFAP, glial fibrillary acidic protein.

*Present address: Department of Anatomy and Neurobiology, Spinal Cord and Brain Injury Research Center, University of Kentucky, Lexington, KY 40506.

†To whom correspondence should be addressed. E-mail: jeffrey_macklis@hms.harvard.edu.

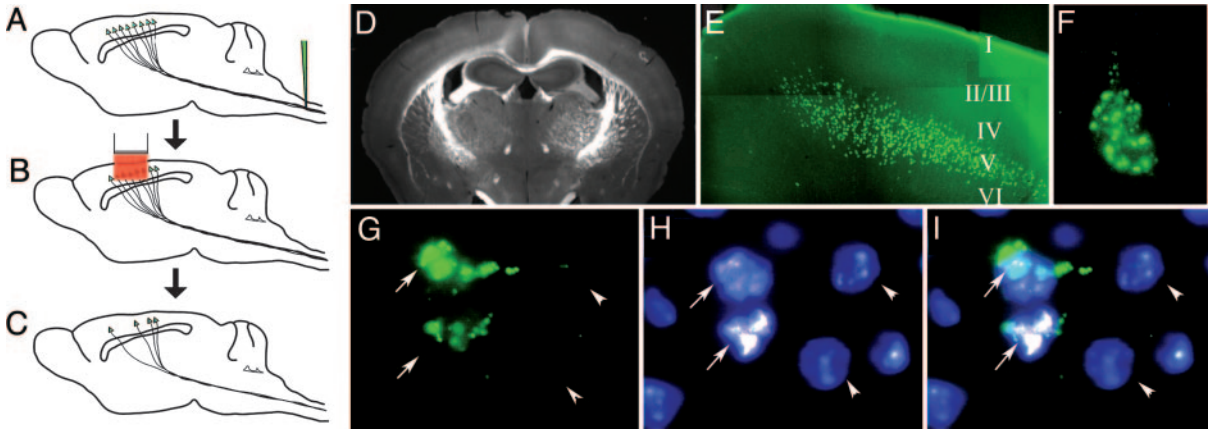


**Fig. 1.** Targeting and induction of CSMN apoptosis. (*A–C*) Schematic of sequential targeting and photoactivation steps to induce CSMN apoptosis. (*A*) Green fluorescent nanospheres carrying chlorin $e_6$ were microinjected into the dorsal spinal cord at the cervical 5–6 level in 4-week-old mice. The nanospheres were retrogradely transported to the somata of layer V CSMN via the corticospinal tract. (*B*) Two weeks later, in mice at 6 weeks of age, we exposed the motor cortex through intact dura to 674-nm-wavelength light collimated at layer V. Photoactivated chlorin $e_6$ produced singlet oxygen within neuronal lysosomes, inducing apoptosis exclusively in nanosphere-containing motor neurons. (*C*) CSMN that both contain nanospheres and are exposed to light undergo selective apoptosis. Surrounding neurons and glia are undamaged. (*D*) Oblique coherent contrast image of a coronal section of anterior brain (Nikon SMZ 1500), indicating location of CSMN. (*E*) Chlorin $e_6$ conjugated green fluorescent nanospheres injected into the cervical spinal cord exclusively label motor neurons in layer V. About 50–60% of the CSMN were targeted by green fluorescent nanospheres carrying chlorin $e_6$. (*F*) Enlarged view of nanosphere-labeled motor neuron in layer V with pyramidal morphology typical of CSMN. Due to the light dosimetry used, degeneration of ≈10–20% of targeted projection neurons occurred. (*G–I*) Targeted CSMN developed pyknotic and fragmented nuclei (arrows), one indication that they were undergoing apoptotic neuronal death. Arrowheads indicate normal nuclei of surrounding healthy neurons. (*G*) CSMN selectively labeled by green photoactive nanospheres 8 days after photoactivation. (*H*) Targeted CSMN developed pyknotic and fragmented nuclei, labeled with Hoechst 33258 in blue (arrows). (*I*) Merged image of *G* and *H*.

in rat anti-BrdUrd (1:100, Harlan Breeders, Indianapolis) and the following primary antibodies: rabbit anti-Doublecortin (anti-Dcx) [1:100, courtesy of J. G. Gleeson (University of California, San Diego) and C. A. Walsh (Harvard Institutes of Medicine, Boston]; mouse anti-NeuN antibody (1:100, Chemicon); rabbit antiglial fibrillary acidic protein (anti-GFAP) (1:100, Sigma). We used highly cross-adsorbed anti-mouse and anti-rabbit Alexa 488 and 546 (Molecular Probes) secondary antibodies to avoid crossreactivity.

**Microscopy.** We performed fluorescence microscopy using a Zeiss Axioplan microscope with high-numerical-aperture immersion objective lenses. We performed confocal microscopy using Noran Instruments (Middleton, WI) Oz and Zeiss LSM 510 laser-scanning confocal microscopes and INTERVISION (Noran Instruments, Middleton, WI) and ZEISS 3D analysis software. We produced 3D digital reconstructions from a series of confocal images taken at 0.5-$\mu$m intervals through the regions of interest.

**Quantification.** We quantified the number of BrdUrd+/NeuN+ neurons in experimental and control regions by sampling every sixth section, using a modified version of the fractionator method (16, 25). We quantified the number of BrdUrd+/FG+ neurons in experimental and control regions by examining all of the sections spanning the motor cortex, 40–50 sections per mouse. To avoid false identification of nuclei of closely apposed newborn glial cells as newborn neuronal nuclei, we added confocal microscopy and 3D reconstructions to modified stereological methods (see ref. 16 and Fig. 5, which is published as supporting information on the PNAS web site). We confirmed the identity of adult-born neurons using confocal microscopy and omitted all cells that had been sectioned to eliminate false positives. These conservative methods likely lead to an underestimate of the true number of neurons generated. The experimental regions of the cortex extended from the dorsal cortex to the medial bank and spanned the thickness of cortical layer V. We compared numbers of new neurons in experimental mice to control mice using the unpaired *t* test with Welch correction, with *P* values $<0.001$ interpreted as demonstrating a significant difference between groups.

**FG Injections.** We microinjected 200 nl of 3% FG solution dissolved in water bilaterally into the dorsal spinal cord at the cervical C2–C3 level at 7, 11, 15, and 55 weeks after induction of targeted CSMN apoptosis. We examined projections formed by newborn neurons 1 week after FG injection.

## Results

To examine whether adult endogenous neural precursors can differentiate into new neurons that extend long-distance projections to the spinal cord, we induced targeted apoptosis of CSMN and examined the progressive differentiation of endogenous precursors. The adult neocortex undergoing targeted apoptosis reexpresses developmental signals that direct transplanted or endogenous precursors to differentiate into neurons (16). We induced synchronous apoptotic degeneration of CSMN in 6-week-old mice via chromophore targeting (Fig. 1) (22, 23, 26, 27). Approximately 10–20% of CSMN underwent apoptosis after successful chromophore targeting. We administered the thymidine analog BrdUrd to the mice for 2 weeks in their drinking water immediately after initiation of neuronal apoptosis and examined the phenotype of newly generated BrdUrd+ cells 2, 4, 8, 12, 16, and 56 weeks after induction of apoptotic degeneration. We examined the differentiation of these cells morphologically and by using markers of developing and mature neurons and glia, including Dcx, NeuN, and GFAP. We also retrogradely labeled CSMN from the cervical spinal cord with FG to investigate whether newborn cortical neurons can project long-distance axons to the spinal cord in the adult CNS.

We first examined the early differentiation of adult-born cells using antibodies to Dcx, a protein expressed exclusively in neurons and preferentially in immature migrating or differentiating neurons (16, 28, 29). The BrdUrd allowed us to establish that the cells were recently born, and the Dcx allowed us to investigate their potential differentiation into neurons. We found adult-born BrdUrd+ cells expressing Dcx only in or underlying the regions of the cortex undergoing targeted CSMN degeneration. In contrast, we did not find any such cells in the cortex of sham-operated control mice. Control mice had BrdUrd+ cells scattered throughout the brain, as

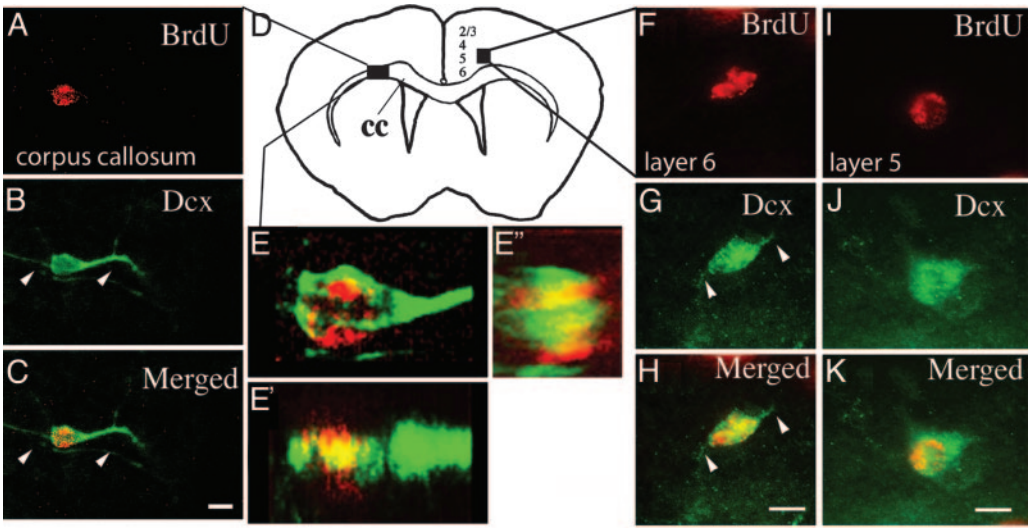


**Fig. 2.** Newborn cells in the cortex adopt a migratory morphology and express the migratory neuronal marker Dcx 2 weeks after induction of apoptosis. Many BrdUrd+/Dcx+ adult-born neurons were located between the corpus callosum and layer 5, appearing to migrate from the SVZ, through the corpus callosum [*A–C*, *E*, *E′*, and *E′′* and layer 6 (*F–H*) and into experimental regions of cortical layer 5 (*I* and *K*)]. (*D*) A drawing of the coronal section for *A–C* shows the position of many Dcx+ newborn neurons in corpus callosum (*A–C*), layer 6 (*F–H*), and layer 5 (*I–K*). Adult-born neurons in experimental cortical layer 6 and underlying corpus callosum exhibit migratory morphology with leading and trailing processes (arrowheads in *B*, *C*, *G*, and *H*). No BrdUrd+/Dcx+ cells were found in corpus callosum or the cortex of control mice. Dcx is preferentially expressed by immature and migratory neurons (26, 27); Dcx staining does not overlap with A2B5, O4, RIP, MBP, or GFAP staining (16). (*A*, *F*, and *I*) BrdUrd+ nuclei are shown in red. (*B*, *G*, and *J*) Dcx+ immature neurons are labeled in green. (*C*, *H*, and *K*) Merged images. (*E*) Confocal analysis confirms that a subset of newborn cells expresses Dcx, a marker of immature, migrating neurons. Laser-scanning confocal images were combined to produce 3D reconstructions of the newborn neurons. Viewing this example, the BrdUrd+/Dcx+ newborn neuron along the *x* (*E′*), *y* (*E″*), and *z* axes (*E*) confirms that the BrdUrd+ nucleus is within the Dcx+ cell body. (*I–K*) Adult-born BrdUrd+/Dcx+ neurons in layer 5 exhibit more mature morphologies, with larger, rounder cell bodies and early extension of dendritic processes typical of pyramidal CSMN. (Bars, 10 $\mu$m.)

expected; however, in the cortex, these cells differentiated into neurons only in regions undergoing targeted apoptosis. No differences were observed in the number of BrdUrd+ cells between control and experimental mice in the cortex or in the SVZ, consistent with previous results (16). Control mice were injected with conjugated nanospheres and underwent a craniotomy and sham exposure to long-wavelength light. Control mice had no BrdUrd+ neurons in the cortex, demonstrating that BrdUrd was not incorporated into mature neurons because of toxicity. In addition, it is extremely unlikely that the BrdUrd+ neurons we observed incorporated BrdUrd while undergoing apoptosis, because (*i*) the BrdUrd+ newborn neurons were never labeled by the original nanospheres; (*ii*) surviving neurons were BrdUrd−; (*iii*) the BrdUrd labeling was dense and uniform, in contrast to light and punctate as seen with DNA repair; and (*iv*) the neurons survived in the neocortex for 1 year after the end of the BrdUrd administration. Furthermore, neurons that had integrated BrdUrd during cell cycle events preceding apoptosis would not survive for >1 year. Neurons labeled with lower levels of the chlorin $e_6$-conjugated nanospheres survive the photoactivating process. These surviving neurons, having undergone sublethal levels of damage, still do not integrate BrdUrd ($n$ = 5,192 cells examined in five mice), demonstrating that this model of apoptosis does not induce BrdUrd integration into preexisting neurons. Furthermore, this model of targeted apoptosis occurs without inducing an inflammatory response (22, 24), gliosis (22–24, 30), or activated cytokine-release-stage microglia (22, 24), as assessed by routine histology, GFAP staining, and F4-80 microglial staining, further confirming that the cellular injury is limited to targeted neurons. As expected, BrdUrd+/Dcx+ cells were present in the SVZ and rostral migratory stream of both experimental and control mice. The BrdUrd+/Dcx+ cells in the cortex of experimental mice extended leading processes, adopting morphologies typical of migrating neurons in the developing brain (Fig. 2). In experimental mice, the migratory morphology and orientation of Dcx+ newborn neurons suggested their migration from the SVZ, through the corpus callosum and neocortical layer VI, and into layer V of the cortex (Fig. 2). No Dcx+ neurons were found in more superficial cortical layers or in the cortex outside the regions undergoing CSMN apoptosis.

To confirm the newborn identity of these Dcx+ neurons and to investigate the unlikely possibility that adult-born cells were merely closely apposed to Dcx+ neurons with migratory morphology, we used laser-scanning confocal microscopy to generate 3D reconstructions of these neurons (Fig. 2 *E*, *E′*, and *E″*). We confirmed that the newborn BrdUrd+ nuclei belong to newborn Dcx+ neurons with migratory morphology. Consistent with the role of Dcx in migration and early differentiation, BrdUrd+/Dcx+ neurons were present in the cortex only soon after the induction of apoptosis at 2 weeks. As the adult-born neurons matured, Dcx expression and migratory morphology were replaced by expression of the mature neuronal marker NeuN and increasingly mature morphology. The finding that BrdUrd+ cells expressed Dcx at early time points, typical of immature migrating and differentiating neurons, demonstrates the appropriate developmental progression of these neurons, further confirming that BrdUrd is appropriately indicating newborn neurons. Together, these results demonstrate that targeted apoptosis of CSMN leads to microenvironmental change that recruits immature neurons to the cortex in a spatially and temporally specific manner.

To determine whether the migratory neuroblasts differentiate into mature neurons in the adult neocortex, we examined the phenotype of adult-born cells morphologically and using antibodies to NeuN, a transcription factor that is expressed in the nucleus and cytoplasm only of mature neurons (31). Newborn BrdUrd+/NeuN+ neurons were found exclusively in regions of layer V of the cortex undergoing apoptotic degeneration of CSMN (Fig. 3 *A–C*; $n$ = 27). We found no adult-born neurons in control mice undergoing craniotomies and sham light exposure ($n$ = 12) or in regions of the cortex that were not targeted to undergo apoptosis, yielding a highly statistically significant difference between control and

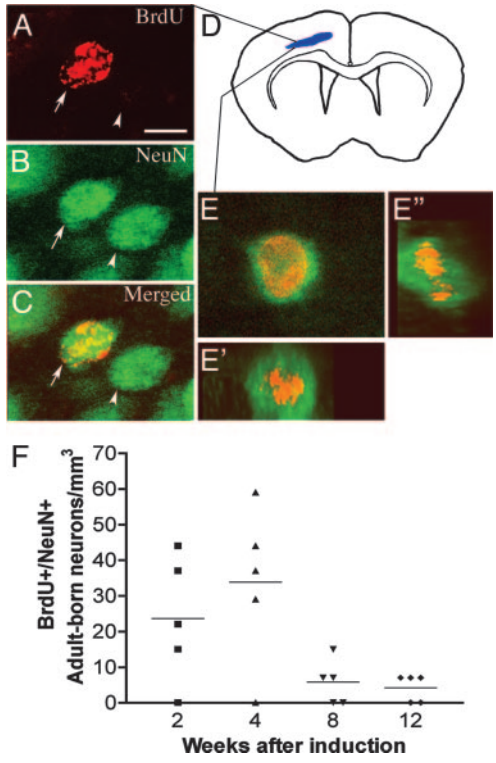


**Fig. 3.** Newly generated BrdUrd+ cells can be induced to differentiate into mature neurons in regions of the cortex undergoing targeted apoptotic CSMN degeneration. (*A–C*) Four weeks after induction of apoptosis, a subset of newborn cells with nuclei labeled with BrdUrd (red; arrow), expressed NeuN (green), a mature neuronal marker. BrdUrd+/NeuN+ neurons had large nuclei typical of mature neurons. Preexisting neurons were not labeled with BrdUrd (arrowhead). (Bar, 10 $\mu$m.) (*C*) Merged image. No BrdUrd+/NeuN+ neurons contained nanospheres, further confirming that they are not preexisting targeted neurons, and that they did not simply integrate BrdUrd because of DNA repair. (*D*) Newborn NeuN+ neurons were exclusively located in layer V of the motor cortex, only in the region that had undergone targeted CSMN apoptosis (blue). (*E*) Laser-scanning confocal images were combined to produce 3D reconstructions of the newborn neurons. Viewing the BrdUrd+/NeuN+ neurons along the *x* (*E''*), *x* (*E'*), and *z* (*E*) axes unequivocally demonstrated the colocalization of BrdUrd and NeuN. (*F*) Quantification of BrdUrd+/NeuN+ adult-born neurons 2, 4, 8, and 12 weeks after induction of CSMN apoptosis. Each point indicates the number of adult-born BrdUrd+/NeuN+ neurons per mm$^3$ in an individual animal; each bar indicates the mean.

experimental mice ($P < 0.001$, unpaired *t* test with Welch correction). To confirm that the adult-born BrdUrd+ cells were truly expressing NeuN, we imaged them using laser-scanning confocal microscopy and produced 3D digital reconstructions (Fig. 3 *E*, *E'*, and *E''*). The results confirm that the adult-born cells are neurons truly expressing NeuN and are not merely newborn glia that are closely apposed to preexisting neurons (see Fig. 5 for an example of such a closely apposed newborn glial cell identified by 3D confocal reconstruction). Some newborn neurons had pyramidal morphology (large 10- to 15-$\mu$m-diameter somata with apical process), characteristic of projection neurons, which extend long-distance axonal projections. These results demonstrate that endogenous neural precursors can be induced *in situ* to differentiate into mature neurons in layer V.

To examine the possibility that these new cells were inappropriately expressing markers of multiple neural phenotypes, we triple-labeled sections with antibodies against the astroglial marker GFAP, in addition to BrdUrd and NeuN. BrdUrd+/NeuN+ neurons never expressed GFAP, confirming that they had differentiated specifically into mature neurons.

We found the greatest number of adult-born neurons 2–4 weeks after induction of apoptosis (Fig. 3*F*). We found 24 ± 17 BrdUrd+/NeuN+ newborn neurons per mm$^3$ in layer V 2 weeks after the induction of apoptosis ($n = 5$) and 34 ± 19 newborn neurons per mm$^3$ 4 weeks after induction ($n = 5$) (Fig. 3*F*). Especially at later survival times, the number of newly recruited newborn neurons was quite variable among experimental animals. We observed 7–15 adult-born neurons per mm$^3$ in three of five experimental animals at 8 weeks after induction and seven adult-born neurons per mm$^3$ in three of five experimental animals at 12 weeks after induction (Fig. 3*F*). Mature adult-born neurons with long-distance projections were still present 56 weeks after induction of apoptosis. These results demonstrate that newborn neurons can be recruited from endogenous neural precursors *in situ*, and that some of these adult-born neurons can survive for >1 year in the cortex. We observed the greatest number of newborn neurons soon after induction of apoptosis and fewer newborn neurons at later times. These results are consistent with patterns of both developmental neurogenesis and adult neurogenesis; more neurons are generated than eventually survive. For example, in the case of olfactory neurogenesis, over half of adult-generated neurons undergo apoptosis in the first 2–3 months after their generation (32, 33). The variability in the number of adult-born neurons generated is at least partially due to the technical challenges involved in injecting nanospheres into the extremely small murine corticospinal tract. Pilot experiments showed that only ≈60% of experimental mice underwent sufficient nanosphere transport to the cortex to induce targeted CSMN apoptosis. We included all experimental mice in our analyses, contributing to the variability in the number of adult-born neurons generated. Successful targeting of corticospinal projection neurons induces endogenous precursors to form mature NeuN-expressing neurons in adult cortex.

A subset of newborn neurons displayed very large pyramidal morphologies, characteristic of CSMN. To further define the identity of the newborn BrdUrd+/NeuN+ neurons and to examine whether these adult-born neurons could reestablish long-distance projections to the spinal cord, we injected the retrograde tracer FG into the cervical spinal cord at level C2–C3 (above the level of the initial chromophore targeting injection) weeks and months after neuronal recruitment. The FG was retrogradely transported and labeled both newborn and original CSMN in layer V of the neocortex (Fig. 4*A*). We investigated potential projections of newborn neurons 8, 12, 16, and 56 weeks after induced synchronous apoptosis of CSMN. At 8 weeks, no projections by newborn CSMN were observed (Fig. 4*I*; $n = 5$), indicating that extension of such long projections takes longer than 8 weeks, consistent with prior results with transplanted neuroblasts (26, 27, 34). At 12 and 16 weeks after neuronal recruitment, we observed a subpopulation of newborn BrdUrd+ neurons that were retrogradely labeled with FG (Fig. 4 *B–G*; $n = 7$), demonstrating that newly recruited adult-born neurons can form axonal projections to the cervical spinal cord. At 56 weeks, one to seven adult-born neurons per mm$^3$ ($n = 5$) maintained long-distance projections to the cervical spinal cord (Fig. 4*I*). We confirmed these results using laser-scanning confocal microscopy and 3D digital reconstructions (Fig. 4 *H*, *H'*, and *H''*, and see Fig. 6, which is published as supporting information on the PNAS web site), demonstrating that the BrdUrd+ nuclei were located completely within the FG+ neuronal cell bodies. The absence of FG+ adult-born neurons at times earlier than 12 weeks further confirms that the BrdUrd is not simply integrating into preexisting neurons; only adult-born neurons that have had enough time to form long-distance projections are both BrdUrd+ and FG+. Newborn neurons progressed sequentially from precursors to Dcx+ migratory neuroblasts to mature NeuN+ neurons without spinal cord projections and finally to mature neurons with projections to the spinal cord. Taken together, these results demonstrate that endogenous neural precursors can be induced to differentiate into mature neurons that form and maintain extremely long-distance

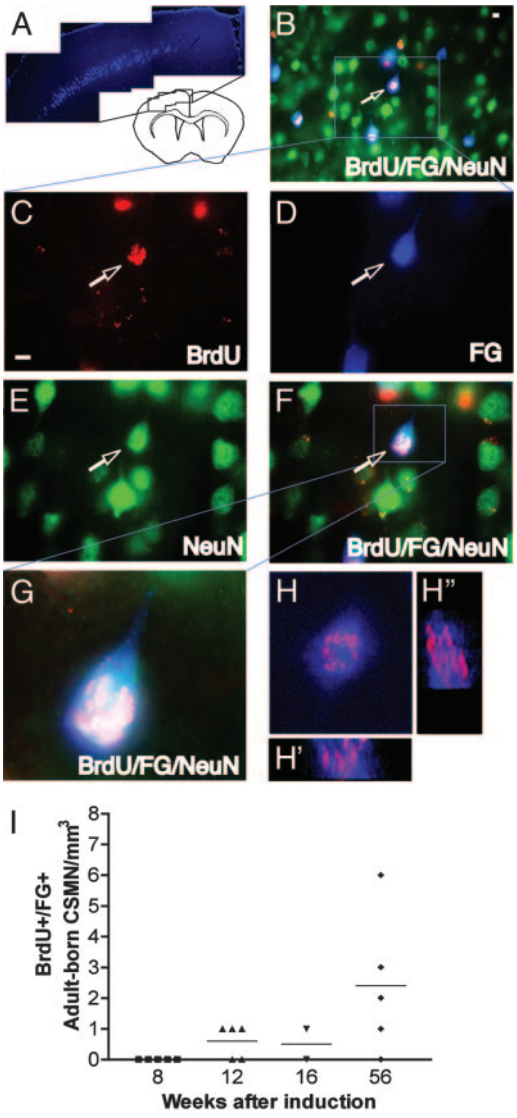


**Fig. 4.** A subset of newborn layer V cortical neurons extends axons to the cervical spinal cord. (*A*) Both newborn and original layer V CSMN were retrogradely labeled by FG (blue). (*B*) Field expanded in *C–F* showing a BrdUrd+/NeuN+/FG+ triple-labeled adult-born neuron (arrow). (Bar, 10 $\mu$m.) (*C–E*) Individual images show that this BrdUrd+ nucleus (*C*; red) is located within this neuron, which is retrogradely labeled with FG from the cervical spinal cord (*D*; blue) and expresses NeuN (*E*; green). (Bar, 10 $\mu$m.) (*F*) Overlay showing BrdUrd+/FG+/NeuN+ neuron colocalization. (*G*) Higher-magnification overlay of the same neuron from *C–F*. (*H*) A separate example of an adult-born neuron with a projection to the spinal cord. Laser-scanning confocal images were combined to produce 3D reconstructions of newborn neurons. Viewing a BrdUrd+/FG+ newborn neuron along its *x* (*H'*), *y* (*H''*), and *z* axes (*H*) unequivocally demonstrates the colocalization of BrdUrd and FG. (*I*) Quantification of BrdUrd+/FG+ adult-born CSMN extending spinal projections from 12 to 56 weeks after induction of original CSMN apoptosis. Each point indicates the number of adult-born BrdUrd+/FG+ neurons per mm$^3$ in an individual animal; each bar indicates the mean.

projections from the motor cortex to the spinal cord over many months.

To further examine the theoretical possibility that preexisting developmentally generated neurons had integrated BrdUrd either because of injury or cell fusion, we labeled existing CSMN before inducing cell death. We injected FG into the cervical spinal cord, retrogradely prelabeling essentially all CSMN. We then injected chromophore-conjugated nanospheres into the cervical spinal cord (additionally labeling preexisting neurons) and, 1 week later, exposed the motor cortex to long-wavelength light, inducing apoptosis of the targeted neurons. Mice were administered BrdUrd and were killed 3 weeks after induction of apoptosis. We could identify essentially all preexisting developmentally generated neurons via FG and the green fluorescent nanospheres. We examined FG- and nanosphere-labeled cells in every 12th section through the motor cortex of five mice. None of the FG-labeled ($n$ = 4,371 cells) or nanosphere-labeled ($n$ = 5,192 cells) neurons contained BrdUrd, unequivocally demonstrating that the BrdUrd+ neurons we identified were not generated by BrdUrd integration due to injury or cell fusion.

## Discussion

There is substantial precedent for neuronal death modifying the fate of immature precursor cells, but until relatively recently, only in regions of the vertebrate brain that have ongoing neurogenesis (35). Recent evidence (16–21) suggests that neuronal death can trigger increased neuron addition in regions of adult CNS that are normally nonneurogenic. Our previous results show that, in regions of the adult mouse neocortex undergoing synchronous apoptotic degeneration of projection neurons, the surrounding cells, including interneurons, up-regulate the expression of a specific set of developmental signaling molecules that may guide neocortical projection neuron differentiation (30). Immature neurons or multipotent neural precursors that are transplanted into these regions migrate selectively to layers of the cortex where projection neurons are degenerating (22, 23, 26, 27). They then differentiate into projection neurons (26, 27), receive afferent synapses (26, 27), and reform appropriate long-distance connections to the original contralateral targets of the degenerating neurons (26). Similarly, induction of targeted neuronal death in projection neurons of the song circuitry in the avian forebrain causes increased neuron replacement from endogenous neural precursors in a system already undergoing low-level neurogenesis (21). In more recent work from our lab, we manipulated endogenous precursors *in situ* to undergo neurogenesis and reformation of corticothalamic connections *de novo* in the adult mouse cortex, where it does not normally occur, by first inducing synchronous apoptotic degeneration of corticothalamic neurons (16). These previous results, regarding both transplantation of immature precursors and induction of adult neocortical neurogenesis, provided support for the hypothesis that manipulation of the local microenvironment by targeted apoptosis of CSMN could induce neurogenesis of this important neuronal population.

Here, our results demonstrate that adult-born CSMN can be generated from endogenous neural precursors and can reform long-distance connections extending from the motor cortex to the spinal cord. Only in regions of the cortex undergoing targeted apoptosis do endogenous precursors, labeled by BrdUrd, enter as migratory neuroblasts and progressively mature into neurons. In our experiments, we gave experimental and control mice drinking water containing BrdUrd after induction of apoptosis. BrdUrd incorporated into dividing cells during S phase to label the newborn cells. The newborn neurons first express the immature neuronal marker Dcx with migratory morphology, then express the mature neuronal marker NeuN with mature pyramidal morphology, and finally form long-distance projections to the spinal cord over a >12-week period.

There are reports that damaged or dying cells can also integrate small amounts of BrdUrd during DNA repair, and that cell fusion with adult neurons can occur (36, 37), suggesting that the simple presence of low-level punctate BrdUrd labeling alone does not unequivocally confirm that a cell is adult-born. Several lines of evidence demonstrate that the neurons we observed were indeed generated during adulthood. First, developmentally generated CSMN labeled with FG before the induction of death do not integrate BrdUrd after cell death. Second, because preexisting projection neurons are also labeled by the fluorescent nanospheres

that carry the targeting chromophore, and because none of the BrdUrd+ cells we observed contained nanospheres, these BrdUrd+/Dcx+ or BrdUrd+/NeuN+ neurons are not preexisting neurons. Conversely, none of the targeted chromophore-containing neurons that survived were BrdUrd+. Third, control mice receiving injections of chromophore-conjugated nanospheres without photoactivation did not contain BrdUrd+ neurons in the cortex, confirming that injection and/or axotomy alone does not lead to BrdUrd incorporation or neuron birth. Fourth, the BrdUrd+ neurons we observed in experimental mice possess dense relatively uniform nuclear BrdUrd staining, not light punctate staining, indicating that they integrated BrdUrd during division and not during DNA repair. In contrast to BrdUrd integrated during cell division, BrdUrd integrated during DNA repair yields a light punctate pattern of BrdUrd staining. Fifth, the BrdUrd+/NeuN+ neurons survive for >1 year, indicating that they did not integrate BrdUrd during pathological mitosis that has been recently reported to sometimes precede the apoptosis of mature neurons (38–40). Sixth, the BrdUrd+/Dcx+ cells we observed possess migratory morphology in the corpus callosum and layer VI underlying targeted region of the cortex; thus, these cannot be pathological preexisting neurons misexpressing Dcx. Taken together, it is extremely unlikely that the BrdUrd+ neurons we observed incorporated BrdUrd while being damaged or undergoing apoptosis. This evidence identifies the BrdUrd+ neurons reported here as adult-born neurons.

Although we observed a significant number of new neurons, the BrdUrd labeling almost certainly underestimates this number, because BrdUrd is available for nuclear incorporation for only a few hours after administration. Although the small number of adult-born neurons observed by using these methods would not be sufficient for functional restoration, it is also possible that the number of recruited CSMN could be increased by enhancing their survival through a critical period until they establish supportive target innervation over weeks to months. In future experiments, it will be of interest to examine the effects of both supporting newborn CSMN survival and enhancing axon outgrowth to targets.

Of particular interest for potential future therapeutic strategies are the possibilities that immature adult-born neurons may be better able to extend axons through the mature or injured CNS than fully mature preexisting neurons. The ability of adult-born neurons to extend appropriate long-distance connections indicates that the adult brain remains capable of supporting axon outgrowth, in contrast to the long-held idea that the adult CNS is absolutely inhibitory to axonal regeneration. The ability of adult-born neurons to reform long-distance projections in these experiments may be in part due to the absence of a glial scar and of up-regulation of inhibitory extracellular matrix proteins, because the local microenvironment was physically unperturbed (e.g., by invasive transplantation techniques) (41). It is also possible that some newborn neurons extend axons to spinal cord by following the existing corticospinal axon fascicles or by extending axons through empty axon paths vacated by axons of neurons induced to undergo apoptosis. It is likely, however, that the ability of newborn neurons to extend axons through the adult CNS is also due to a combination of a prolonged neuron-intrinsic phase of developmentally regulated axon extension (42) and a relative lack of receptors to myelin-associated growth-inhibitory molecules (43). It might be of interest to examine whether immature adult-born neurons can extend their axons through the regions of glial scarring associated with spinal cord injury better than mature preexisting neurons.

It may be possible to use growth factors affecting proliferation, differentiation, and/or survival to increase the efficiency of the neurogenesis reported here. Growth factor enhancement of proliferation of endogenous neural precursors might increase the number of adult-born neurons initially generated, but simply increasing the number of neurons generated would not be sufficient to achieve functional neuronal circuit repair. Newly generated neurons must survive and form appropriate connections. Extending the survival of adult-born neurons via specific growth factor manipulation might allow neurons more time to form appropriate connections from which they might receive target-derived factors necessary for their survival. Consistent with this idea is our finding that the number of adult-born neurons initially present in the cortex decreases with time until they reach the cervical spinal cord, suggesting that adult-born neurons that do not receive proper survival signals undergo apoptosis, just as occurs during initial cortical development.

Taken together, these results demonstrate that endogenous precursors can generate even the highly complex CSMN in the adult cortex, and that it is possible for these neurons to form long-distance projections to the adult mouse spinal cord. Further understanding the potential of endogenous neural precursors and controls over their lineage-specific differentiation may allow the development of more efficient neuronal replacement therapies that do not depend on transplantation of exogenous cells.

This work was partially supported by grants from the National Institutes of Health and the Christopher Reeve Paralysis Foundation (to J.D.M.). Some confocal imaging was performed in facilities supported by the Harvard Center for Neurodegeneration and Repair.

1. Gage, F. H. (2000) *Science* **287,** 1433–1438.
2. Temple, S. (2001) *Nature* **414,** 112–117.
3. Temple, S. & Alvarez-Buylla, A. (1999) *Curr. Opin. Neurobiol.* **9,** 135–141.
4. Reynolds, B. A. & Weiss, S. (1992) *Science* **255,** 1707–1710.
5. Richards, L. J., Kilpatrick, T. J. & Bartlett, P. F. (1992) *Proc. Natl. Acad. Sci. USA* **89,** 8591–8595.
6. Doetsch, F., Garcia-Verdugo, J. M. & Alvarez-Buylla, A. (1997) *J. Neurosci.* **17,** 5046–5061.
7. Van Praag, H., Schinder, A. F., Christie, B. R., Toni, N., Palmer, T. D. & Gage, F. H. (2002) *Nature* **415,** 1030–1034.
8. Kempermann, G. & Gage, F. H. (2002) *Brain Res. Dev. Brain Res.* **134,** 1–12.
9. Van Praag, H., Kempermann, G. & Gage, F. H. (1999) *Nat. Neurosci.* **2,** 266–270.
10. Kempermann, G., Kuhn, H. G. & Gage, F. H. (1997) *Nature* **386,** 493–495.
11. Shingo, T., Gregg, C., Enwere, E., Fujikawa, H., Hassam, R., Geary, C., Cross, J. C. & Weiss, S. (2003) *Science* **299,** 117–120.
12. Parent, J. M. & Lowenstein, D. H. (2002) *Prog. Brain Res.* **135,** 121–131.
13. Parent, J. M., Yu, T. W., Leibowitz, R. T., Geschwind, D. H., Sloviter, R. S. & Lowenstein, D. H. (1997) *J. Neurosci.* **17,** 3727–3738.
14. Kempermann, G. & Kronenberg, G. (2003) *Biol. Psychiatry* **54,** 499–503.
15. Kuhn, H. G., Dickinson-Anson, H. & Gage, F. H. (1996) *J. Neurosci.* **16,** 2027–2033.
16. Magavi, S. S., Leavitt, B. R. & Macklis, J. D. (2000) *Nature* **405,** 951–955.
17. Nakatomi, H., Kuriu, T., Okabe, S., Yamamoto, S., Hatano, O., Kawahara, N., Tamura, A., Kirino, T. & Nakafuku, M. (2002) *Cell* **110,** 429–441.
18. Arvidsson, A., Collin, T., Kirik, D., Kokaia, Z. & Lindvall, O. (2002) *Nat. Med.* **8,** 963–970.
19. Parent, J. M., Vexler, Z. S., Gong, C., Derugin, N. & Ferriero, D. M. (2002) *Ann. Neurol.* **52,** 802–813.
20. Zhao, M., Momma, S., Delfani, K., Carlen, M., Cassidy, R. M., Johansson, C. B., Brismar, H., Shupliakov, O., Frisen, J. & Janson, A. M. (2003) *Proc. Natl. Acad. Sci. USA* **100,** 7925–7930.
21. Scharff, C., Kirn, J. R., Grossman, M., Macklis, J. D. & Nottebohm, F. (2000) *Neuron* **25,** 481–492.
22. Sheen, V. L. & Macklis, J. D. (1995) *J. Neurosci.* **15,** 8378–8392.
23. Macklis, J. D. (1993) *J. Neurosci.* **13,** 3848–3863.
24. Sheen, V. L. & Macklis, J. D. (1994) *Exp. Neurol.* **130,** 67–81.
25. Guillery, R. W. & Herrup, K. (1997) *J. Comp. Neurol.* **386,** 2–7.
26. Fricker-Gates, R. A., Shin, J. J., Tai, C. C., Catapano, L. A. & Macklis, J. D. (2002) *J. Neurosci.* **22,** 4045–4056.
27. Shin, J. J., Fricker-Gates, R. A., Perez, F. A., Leavitt, B. R., Zurakowski, D. & Macklis, J. D. (2000) *J. Neurosci.* **20,** 7404–7416.
28. Gleeson, J. G., Lin, P. T., Flanagan, L. A. & Walsh, C. A. (1999) *Neuron* **23,** 257–271.
29. Francis, F., Koulakoff, A., Boucher, D., Chafey, P., Schaar, B., Vinet, M. C., Friocourt, G., McDonnell, N., Reiner, O., Kahn, A., *et al.* (1999) *Neuron* **23,** 247–256.
30. Wang, Y., Sheen, V. L. & Macklis, J. D. (1998) *Exp. Neurol.* **154,** 389–402.
31. Mullen, R. J., Buck, C. R. & Smith, A. M. (1992) *Development (Cambridge, U.K.)* **116,** 201–211.
32. Winner, B., Cooper-Kuhn, C. M., Aigner, R., Winkler, J. & Kuhn, H. G. (2002) *Eur. J. Neurosci.* **16,** 1681–1689.
33. Petreanu, L. & Alvarez-Buylla, A. (2002) *J. Neurosci.* **22,** 6106–6113.
34. Hernit-Grant, C. S. & Macklis, J. D. (1996) *Exp. Neurol.* **139,** 131–142.
35. Parent, J. M. (2003) *Neuroscientist* **9,** 261–272.
36. Alvarez-Dolado, M., Pardal, R., Garcia-Verdugo, J. M., Fike, J. R., Lee, H. O., Pfeffer, K., Lois, C., Morrison, S. J. & Alvarez-Buylla, A. (2003) *Nature* **425,** 968–973.
37. Weimann, J. M., Charlton, C. A., Brazelton, T. R., Hackman, R. C. & Blau, H. M. (2003) *Proc. Natl. Acad. Sci USA* **100,** 2088–2093.
38. Yang, Y., Geldmacher. D. S. & Herrup, K. (2003) *J. Neurosci.* **21,** 2661–2668.
39. Konishi, Y & Bonni, A. (2003) *J. Neurosci.* **23,** 1649–1658.
40. Katchanov, J. Katchanov, J., Harms, C., Gertz, K., Hauck, L., Waeber, C., Hirt, L., Priller, J., von Harsdorf, R., Bruck, W., *et al.* (2001) *J. Neurosci.* **21,** 5045–5053.
41. Grimpe, B. & Silver, J. (2004) *J. Neurosci.* **24,** 1393–1397.
42. Tessier-Lavigne, M. & Goodman, C. S. (1996) *Science* **274,** 1123–1133.
43. Oertle, T. & Schwab, M. E. (2003) *Trends Cell Biol.* **13,** 187–194.